

# Pulsed Plasma Deposition of Super-Hydrophobic Nanospheres

D. O. H. Teare, C. G. Spanos, P. Ridley, E. J. Kinmond, V. Roucoules, and  
J. P. S. Badyal\*

Department of Chemistry, Science Laboratories, Durham University,  
Durham DH1 3LE, England, UK

S. A. Brewer, S. Coulson, and C. Willis

DSTL, Porton Down, Salisbury SP4 OJQ, England, UK

Received November 7, 2001. Revised Manuscript Received February 6, 2002

Repetitive bursts of continuous wave plasma polymerization on the minute time scale are found to lead to the deposition of well-defined polymeric nanospheres. This unique mode of film growth is attributed to a high level of monomer replenishment in combination with minimal secondary reaction processes (e.g., fragmentation, cross-linking, and etching). In the case of the 1H,1H,2H,2H-perfluorooctyl acrylate precursor, high contact angle (super-hydrophobic) surfaces are produced by this method.

## Introduction

Liquid repellent surfaces are important for many technological applications including biocompatibility,<sup>1</sup> protective coatings,<sup>2</sup> and stain-resistant finishes.<sup>3</sup> The liquid repellency of a surface is principally governed by a combination of its chemical nature (i.e. surface energy) and topographical microstructure (roughness). For instance, although flat low surface energy materials tend to exhibit high water contact angle values,<sup>4</sup> this is normally insufficient to produce super-hydrophobicity (this description is reserved for materials upon which water droplets move spontaneously or easily across horizontal or near horizontal surfaces<sup>5,6</sup>). To achieve super-hydrophobicity, the difference between the advancing and the receding water contact angles (contact angle hysteresis) must be minimal. This is because contact angle hysteresis is effectively an indication of the force required to move a liquid droplet across the surface (i.e., in the case of little or no hysteresis, very little force is sufficient to move the droplet; hence, it easily rolls off<sup>7,8</sup>). One way of lowering contact angle hysteresis is to roughen the substrate.<sup>9</sup> Theory predicts that for idealized rough hydrophobic surfaces, contact

angle hysteresis rises with increasing surface roughness up to a maximum value;<sup>10</sup> roughness levels exceeding this optimum level cause a drop in contact angle hysteresis attributable to the formation of a composite interface (where the liquid does not completely penetrate the surface). Roughness length scales below approximately 30  $\mu\text{m}$  are prerequisite for super-hydrophobicity.<sup>11</sup>

In this context, a variety of methods have been reported for creating super-hydrophobic (roughened low contact angle hysteresis) surfaces. These include sublimation of aluminum acetylacetone from boehmite, titania, or silica coatings;<sup>3,12</sup> sol–gel deposition of alumina and silica;<sup>13,14</sup> anodic oxidation of aluminum;<sup>6</sup> and photolithographically etched surfaces.<sup>11</sup> All of these systems involve a preroughening step followed by functionalization with a fluoroalkyl (low surface energy) coupling agent. Other approaches have included embedding PTFE oligomer particles into nickel electrodes,<sup>15</sup> compressing submicrometer particles,<sup>5</sup> and plasma-based etching<sup>16</sup> or deposition<sup>17</sup> techniques. Plasma etching tends to be limited to low surface energy substrates, whereas plasma deposition is adaptable to a wide range of materials. Some examples of liquid repellent films prepared by the latter technique include the plasma polymerization of vinylidene fluoride,<sup>18</sup>

\* To whom correspondence should be addressed.

(1) Busscher, H. J.; Stokroos, I.; Golverdingen, J. G.; Schakenraad, J. M. *Cells Mater.* **1991**, *1*, 243.  
(2) Alessandrini, G.; Aglietto, M.; Castelvetro, V.; Ciardelli, F.; Peruzzi, R.; Toniolo, L. J. *Appl. Polym. Sci.* **2000**, *76*, 962.  
(3) Nakajima, A.; Hashimoto, K.; Watanabe, T.; Takai, K.; Yamuchi, G.; Fujishima, A. *Langmuir* **2000**, *16*, 7044.  
(4) Tsibouklis, J.; Graham, P.; Eaton, P. J.; Smith, J. R.; Nevell, T. G.; Smart, J. D.; Ewen, R. J. *Macromolecules* **2000**, *33*, 8460.  
(5) Chen, W.; Fadeev, A. Y.; Hsieh, M. C.; Oner, D.; Youngblood, J.; McCarthy, T. J. *Langmuir* **1999**, *15*, 3395.  
(6) Shibuichi, S.; Yamamoto, T.; Onda, T.; Tsuji, K. *Journal of Colloid and Interface Science* **1998**, *208*, 287.  
(7) Furmidge, C. G. L. *J. Colloid Sci.* **1962**, *17*, 309.  
(8) Miwa, M.; Nakajima, A.; Fujishima, A.; Hashimoto, K.; Watanabe, T. *Langmuir* **2000**, *16*, 5754.  
(9) Nakajima, A.; Hashimoto, K.; Watanabe, T. *Monatsh. Chem.* **2001**, *132*, 31.

(10) Johnson, R. E.; Dettre, R. H. *Adv. Chem. Ser.* **1964**, *43*, 112.  
(11) Oner, D.; McCarthy, T. J. *Langmuir* **2000**, *16*, 7777.  
(12) Nakajima, A.; Fujishima, A.; Hashimoto, K.; Watanabe, T.; *Adv. Mater.* **1999**, *16*, 1365.  
(13) Tadanaga, K.; Morinaga, J.; Matsuda, A.; Minami, T. *Chem. Mater.* **2000**, *12*, 590.  
(14) Hong, B. S.; Han, J. H.; Kim, S. T.; Cho, Y. J.; Park, M. S.; Dolukhanyan, T.; Sung, C. *Thin Solid Films* **1999**, *351*, 274.  
(15) Kunugi, Y.; Nonaku, T.; Chong, Y. B.; Watanabe, N. *J. Electroanal. Chem.* **1993**, *353*, 209.  
(16) Busscher, H. J.; Stokroos, I.; Vandermei, H. C.; Rouxhet, P. G.; Schakenraad, J. M. *J. Adhes. Sci. Technol.* **1992**, *6*, 347.  
(17) Youngblood, J. P.; McCarthy, T. J. *Macromolecules* **1999**, *32*, 6800.  
(18) Sato, D.; Jikei, M.; Kakimoto, M. *Polym. Prepr.* **1998**, *39*, 926.

tetrafluoroethylene,<sup>19</sup> fluoroalkylsilanes,<sup>20</sup> and long chain fluorinated alkene and acrylate precursors.<sup>21–24</sup>

In this article we show how a careful choice of plasma polymerization parameters can lead to the growth of low surface energy films that display super-hydrophobicity (low contact angle hysteresis). It is found that pulsing the deposition of the 1H,1H,2H,2H-perfluoroctyl acrylate ( $\text{H}_2\text{C}=\text{CHCO}_2\text{CH}_2\text{CH}_2(\text{CF}_2)_5\text{CF}_3$ , PFAC) plasma polymer on the minute (rather than the micro- to millisecond<sup>22</sup>) time scale leads to a significant enhancement of super-hydrophobicity due to nanosphere formation. These surfaces have been characterized by contact angle analysis, X-ray photoelectron spectroscopy (XPS), infrared spectroscopy, time-of-flight secondary ion mass spectroscopy (ToF-SIMS), and atomic force microscopy (AFM).

## Experimental Section

Plasma polymerization experiments were carried out in a electrodeless cylindrical glass reactor with an externally wound copper coil for RF power coupling (7.8 cm diameter, 2.1 dm<sup>3</sup> volume). This was evacuated by a two-stage Edwards rotary pump connected to a liquid nitrogen cold trap (base pressure and leak rate better than  $2 \times 10^{-3}$  mbar and  $4.8 \times 10^{-10}$  mol s<sup>-1</sup>, respectively). The system pressure was monitored by a Pirani gauge. The standing wave ratio (SWR) of power transmitted to the electrical discharge from a 13.56 MHz radio frequency (rf) generator was optimized using an L-C matching circuit. Prior to each experiment, the reactor was cleaned by scrubbing with detergent and rinsing in water and propan-2-ol, followed by oven-drying. Next, an air-cleaning plasma was run at 0.3 mbar pressure and 40 W power for 30 min. The system was then vented to atmosphere, and a glass substrate slide (ultrasonically cleaned in a 1:1 mixture of propan-2-ol and cyclohexane) was inserted into the center of the chamber, followed by pumping back down to base pressure. At this stage, monomer vapor (1H,1H,2H,2H-perfluoroctyl acrylate, Fluorochem +95%, further purified using multiple freeze–pump–thaw cycles) was introduced at a pressure of 0.25 mbar and the system was allowed to purge for at least 5 min prior to ignition of the electrical discharge at 40 W. In the case of repetitive plasma depositions, monomer flow was maintained throughout (including the 2 min between each reignition of the glow discharge). Upon completion of the last deposition, the monomer feed was valved off after a further 5 min purge, and then the chamber was pumped down to base pressure prior to venting to atmosphere.

Sessile drop contact angle values were acquired using a video capture apparatus (A.S.T. Products VCA2500XE). Water and *n*-decane were chosen as the probe liquids for hydrophobicity and oleophobility, respectively. For each measurement, a 2  $\mu\text{L}$  droplet was dispensed onto the substrate under investigation. Super-hydrophobicity was identified in cases where the water droplet did not adhere to the surface (i.e. rolled off). Contact angle hysteresis values were obtained by lowering a liquid droplet toward the underlying surface until it just touched (without any distortion of the circular shape). Advancing contact angle measurements were then made by increasing the droplet volume (thus pushing the droplet against the solid surface). Likewise, receding contact angle values were determined by withdrawing liquid from the droplet.<sup>25</sup>

- (19) Washo, B. D. *Org. Coat. Appl. Polym. Sci. Proc.* **1982**, *47*, 69.
- (20) Hozumi, A.; Takai, O. *Thin Solid Films* **1997**, *303*, 222.
- (21) Coulson, S. R.; Woodward, I.; Badyal, J. P. S.; Brewer, S. A.; Willis, C. *J. Phys. Chem. B* **2000**, *104*, 8836.
- (22) Coulson, S. R.; Woodward, I. S.; Badyal, J. P. S.; Brewer, S. A.; Willis, C. *Chem. Mater.* **2000**, *12*, 2031.
- (23) Coulson, S. R.; Woodward, I. S.; Badyal, J. P. S.; Brewer, S. A.; Willis, C. *Langmuir* **2000**, *16*, 6287.
- (24) Hsieh, M. C.; Chen, W.; McCarthy, T. J. *Polym. Prepr.* **1999**, *40*, 549.

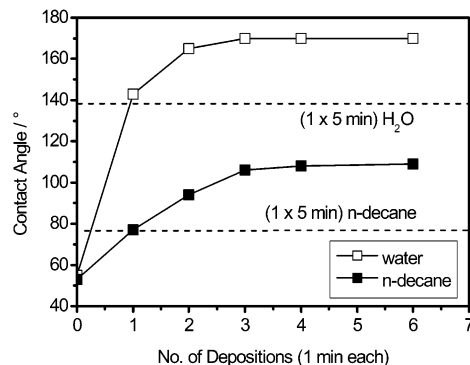


**Figure 1.** Water and *n*-decane sessile drop contact angles for 1H,1H,2H,2H-perfluoroctyl acrylate plasma polymer films.

A VG ESCALAB MKII electron spectrometer equipped with a nonmonochromated Mg K $\alpha$  X-ray source (1253.6 eV) and a hemispherical analyzer operating in CAE mode (20 eV pass energy) was used for X-ray photoelectron spectroscopy (XPS). XPS core level spectra were fitted using Marquardt minimization computer software assuming a linear background and equal full-width at half-maximum (fwhm). Elemental compositions were calculated using instrument sensitivity (multiplication) factors determined from chemical standards; C(1s):O(1s):F(1s) equals 1.00:0.36:0.24. The absence of any Si(2p) signal from the coated glass substrate was taken as being indicative of a continuous coating layer of at least 5 nm thickness.

Fourier transform infrared (FTIR) analysis of plasma deposited films onto potassium bromide plates was carried out on a Perkin-Elmer Spectrum 1 spectrometer fitted with an attenuated total reflection accessory (Graseby Specac Golden Gate). The instrument was operated at 4 cm<sup>-1</sup> resolution in conjunction with a liquid nitrogen cooled MCT detector.

Time-of-flight secondary ion mass spectrometry (ToF-SIMS) analysis was carried out with a Physical Electronics 7200 instrument, which has been described elsewhere.<sup>26</sup> The primary ion beam (8 keV Cs<sup>+</sup>) was focused to a spot size of  $\sim$ 50  $\mu\text{m}$  and rastered over an area of  $100 \times 100 \mu\text{m}$ , and the total dose was kept well under  $10^{13}$  ions  $\text{cm}^{-2}$  (static conditions).<sup>27</sup>

Atomic force microscopy (AFM) images of the plasma polymer surfaces were taken using a Nanoscope III (Digital Instruments) operating in tapping mode (in order to minimize sample damage). Particle size analysis was carried out using Scion Image software (version Beta 4.0.2.).

## Results

Sessile drop water contact angle measurements revealed that repetitive short depositions of PFAC plasma polymer gave rise to greater super-hydrophobicity compared to the equivalent continuous deposition corresponding to a summation of all the individual depositions (Figure 1). Each short burst of plasma deposition lasted 1 min, followed by a 2 min period of monomer purging. Four “bursts” of 1 min duration ( $4 \times 1$  min) were found to be sufficient to produce a super-hydrophobic coating (defined by a static water contact angle greater than 160°, as well as low contact angle hysteresis<sup>5,17</sup>). No significant improvement in super-hydrophobicity was found for additional deposition bursts. A control experiment using a single 5 min deposition ( $1 \times 5$  min) gave a lower water contact angle value of 139°. A related set of measurements were carried out using

- (25) Johnson, R. E.; Dettre, R. H. In *Wettability*; Berg, J. C., Ed.; Marcel Dekker: New York, 1993; Chapter 1, p 13.
- (26) Reichlmaier, S.; Hammond, J. S.; Hearn, M. J.; Briggs, D. *Surf. Interface Anal.* **1994**, *21*, 739.
- (27) Briggs, D. In *Practical Surface Analysis*, 2nd ed.; Briggs, D., Seah, M. P., Eds.; John Wiley & Sons: New York, 1992; Vol. 2.

**Table 1. Advancing and Receding Contact Angles on 1H,1H,2H,2H-Perfluoroctyl Acrylate Plasma Polymer Surfaces**

deposition	contact angle/deg			
	water		<i>n</i> -decane	
	advancing	receding	advancing	receding
5 × 1 min	168 ± 0.8	165 ± 1.2	105 ± 1.0	42 ± 1.7
1 × 5 min	145 ± 1.2	47 ± 1.5	80 ± 1.4	32 ± 1.3

**Table 2. XPS Elemental Compositions of 1H,1H,2H,2H-Perfluoroctyl Acrylate Plasma Polymer Surfaces**

no. of depositions	% C	% F	% O
1 × 1 min	42.0 ± 0.1	49.3 ± 3.5	8.7 ± 2.5
2 × 1 min	41.7 ± 1.1	51.0 ± 2.0	7.6 ± 1.0
4 × 1 min	41.6 ± 2.4	52.0 ± 1.8	6.3 ± 1.1
6 × 1 min	41.8 ± 0.8	51.4 ± 0.4	6.8 ± 0.4
1 × 5 min	42.0 ± 0.6	50.6 ± 0.1	7.4 ± 0.4
monomer	42.3	50.0	7.7

*n*-decane as the probe liquid, to examine the oleophobic characteristics of these deposited films (Figure 1). In this case a plateau around 110° was reached after 4 × 1 min depositions, and further 1 min depositions yielded no further improvement in liquid repellency. For comparison, the 1 × 5 min continuous deposition gave a lower *n*-decane contact angle value of only 77°.

Advancing and receding water contact angle measurements obtained for the 5 × 1 min deposition PFAC plasma polymer films indicated very little hysteresis (thus confirming super-hydrophobicity), whereas considerable hysteresis was observed for the 1 × 5 min coating (Table 1). A large hysteresis was also evident for the *n*-decane probe liquid under both types of plasma deposition conditions (as well as smaller advancing and receding contact angle values, in accordance with the lower surface tension of *n*-decane compared to water<sup>28</sup>).

XPS analysis of the *n* × 1 min and 1 × 5 min PFAC plasma polymer surfaces gave carbon, oxygen, and fluorine elemental abundances that were very similar to the stoichiometry of the PFAC monomer (Table 2). However, subtle differences were evident in the accompanying high-resolution C(1s) envelopes (Figure 2). These could be fitted to seven different types of carbon environment:<sup>29</sup> C-C/C-H (hydrocarbon) at 285.0 eV, C-CF<sub>x</sub> (hydrocarbon adjacent to a fluorocarbon group) at 285.4 eV, C-O at 286.6 eV, C=O at 287.8 eV, CF or O-C=O (ester or carboxylic acid) at 289.4 eV, CF<sub>2</sub> at 291.3 eV, and CF<sub>3</sub> at 293.4 eV. Additional Mg K<sub>3,4</sub> X-ray satellite peaks, shifted by ~9 eV toward lower binding energy, were also taken into consideration. The amount of fluorinated carbon species at the surface was found to increase with the number of 1 min depositions, ranging from approximately 48% ± 1.0 CF<sub>x=2,3</sub> groups for 1 × 1 min deposition to around 55% ± 2.6 of the total C(1s) content for 6 × 1 min deposition. The latter value closely matches the expected monomer stoichiometry of 54.6% total CF<sub>x</sub> content. The amount of fluorinated carbon for the 1 × 5 min deposition was slightly lower at 52% ± 0.6 CF<sub>x=2,3</sub>.

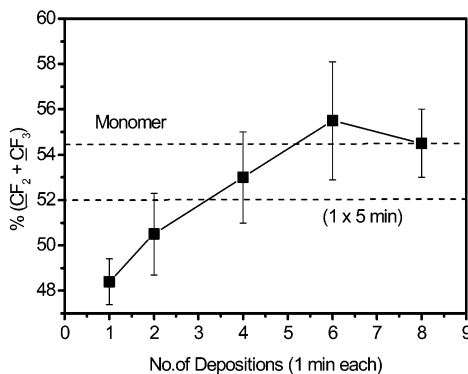


**Figure 2.** Effect of sequential plasma depositions on the concentration of CF<sub>2</sub> and CF<sub>3</sub> groups present in the C(1s) XPS spectra.

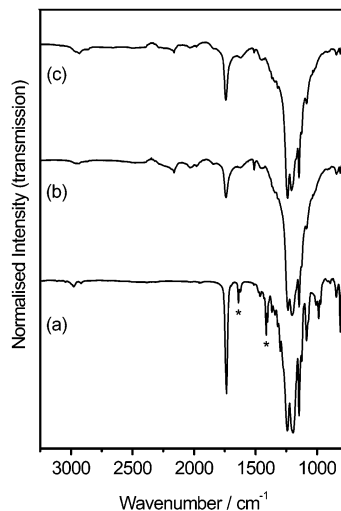


**Figure 3.** Infrared spectra of 1H,1H,2H,2H-perfluoroctyl acrylate: (a) monomer; (b) ATR-FTIR of 5 × 1 min super-hydrophobic plasma polymer; and (c) ATR-FTIR of 1 × 5 min plasma polymer (\* indicates C=C bond absorbances).

Infrared spectroscopy showed that the characteristic C=C bond absorbances at 1638 and 1412 cm<sup>-1</sup> associated with the PFAC monomer disappeared during plasma polymerization (Figure 3), while C-F (1240–1145 cm<sup>-1</sup>), C=O ester (1735 cm<sup>-1</sup>), and C-H (2940 cm<sup>-1</sup>) groups were still evident.

ToF-SIMS analysis of the super-hydrophobic PFAC plasma polymer films identified typical mass fragments associated with perfluoroalkyl chains<sup>30,31</sup> (for both positive and negative ion spectra) (Figure 4 and Table 3). The repetition of peaks every 50 mass units in the positive ion spectrum at *m/z* = 69, 119, 169, and 219 is indicative of  $-(CF_2)_nCF_3$  groups, where *n* = 0, 1, 2, and 3, respectively. The peaks denoted B are representative of up to six fluorinated carbons with a terminal alkene, while the A fragments are probably smaller fluorinated chains with a terminal hydroxyl group. The peak denoted C corresponds to an intact perfluorocarbon chain belonging to the PFAC monomer. There are also features attributable to the incorporation of whole monomer repeat units, these start from *m/z* =

(28) Jasper, J. J. *J. Phys. Chem. Ref. Data* **1972**, *1*, 841.

(29) Beaman, G.; Briggs, D. *High-Resolution XPS of Organic Polymers, The Scienta ESCA 300 Database*; John Wiley & Sons: New York, 1992.

(30) Castner, D. G.; Lewis, K. B.; Fischer, D. A.; Ratner, B. D.; Gland, J. L.; *Langmuir* **1993**, *9*, 537.

(31) Thomas, R. R.; Anton, D. R.; Graham, W. F.; Darmon, M. J.; Saver, B. B.; Stika, K. M.; Swartzfager, D. G. *Macromolecules* **1997**, *30*, 2883.

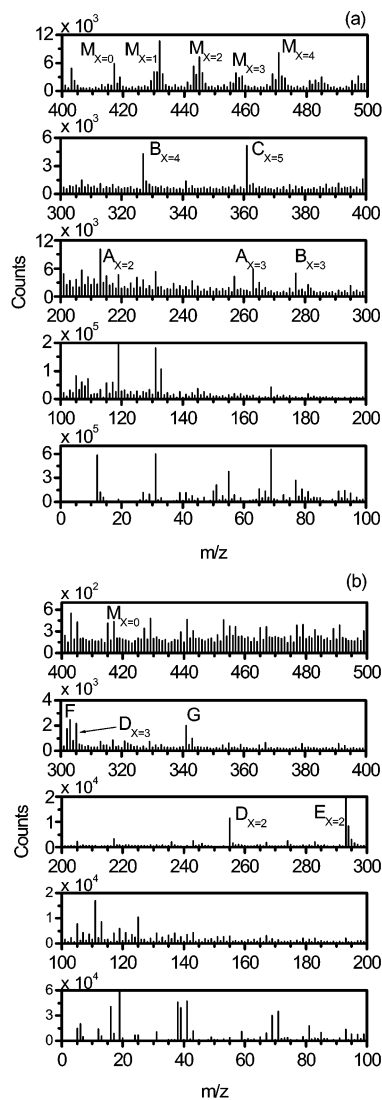


**Figure 4.** ToF-SIMS spectra of  $5 \times 1$  min super-hydrophobic  $1H,1H,2H,2H$ -perfluoroctyl acrylate plasma polymer: (a) positive ion spectrum and (b) negative ion spectrum.

418 ( $M_{x=0}$ , the monomer molecular mass), with related peaks corresponding to additional  $\text{CH}/\text{CH}_2$  groups ( $m/z = 432$  ( $M_{x=1}$ ), 445 ( $M_{x=2}$ ), 458 ( $M_{x=3}$ ), 471 ( $M_{x=4}$ ), etc.). Above  $m/z = 600$ , there are no significant peaks until  $m/z = 766$  (two monomer units with a  $\text{CF}_3$  group missing). In the negative ion spectrum, the peak at  $m/z = 19$  is due to fluorine, and the prominent peak marked E can be assigned to an acetylidy-type fragment<sup>31</sup> (other fragments of this type are labeled as peaks marked D). The peaks G and  $D_{x=3}$  both contain six fluorinated units in their structure. Additional fragments were identified at  $m/z = 527$  and 821. Overall, these ToF-SIMS spectra portray the longest perfluorocarbon chain as containing six fluorocarbon centers, which is consistent with the parent PFAC monomer structure.

Atomic force microscopy images of the  $5 \times 1$  min PFAC plasma polymer surface revealed a globular morphology (Figure 5). On the microscopic scale, these surfaces are extremely rough due to their particulate structure. The particle size distribution for these coatings was quantified using AFM image analysis software. This revealed a mean particle diameter of  $0.52 \mu\text{m}$  with a range spanning  $0.3\text{--}1 \mu\text{m}$  (Figure 6). In contrast, the  $1 \times 5$  min PFAC plasma polymer film contains poorly

**Table 3. Structural Assignments of ToF-SIMS Molecular Fragments**

Peak	Positive Spectrum		Negative Spectrum	
	Proposed Structure	Peak	Proposed Structure	Peak
213 A $x=2$	$\text{CF}_3\left(\text{CF}_2\right)_x\text{CH}_2\overset{+}{\text{CH}}\text{OH}$	255 D $x=2$	$\text{CF}_3\left(\text{CF}_2\right)_x\text{CF}=\text{CF}-\text{C}\equiv\text{C}$	
263 A $x=3$	$\text{CF}_3\left(\text{CF}_2\right)_x\text{CH}_2\overset{+}{\text{CH}}\text{OH}$	293 E $x=2$	$\text{CF}_3\left(\text{CF}_2\right)_x\text{CF}_2-\text{CF}_2-\text{C}\equiv\text{C}$	
277 B $x=3$	$\text{CF}_3\left(\text{CF}_2\right)_x^+\text{CF}-\text{CH}=\text{CH}_2$	303 F $x=3$	$\text{CF}_3\left(\text{CF}_2\right)_x\text{CF}-\text{CF}=\text{C}=\text{C}\text{H}$	
327 B $x=4$	$\text{CF}_3\left(\text{CF}_2\right)_x^+\text{CF}-\text{CH}=\text{CH}_2$	305 D $x=3$	$\text{CF}_3\left(\text{CF}_2\right)_x\text{CF}=\text{CF}-\text{C}\equiv\text{C}$	
361 C $x=5$	$\text{CF}_3\left(\text{CF}_2\right)_x\text{CH}=\overset{+}{\text{C}}-\text{OH}$	341 G $x=3$	$\text{CF}_3\left(\text{CF}_2\right)_x\text{CF}_2-\text{CF}=\text{C}=\text{C}\text{H}$	
418 M $x=0$	$\text{CF}_3\left(\text{CF}_2\right)_5\text{CH}_2-\text{CH}_2-\overset{\text{O}}{\underset{\text{Y}=1\text{ or }2}{\text{C}}}-\text{CH}-\text{CH}_2-\left(\text{CH}_2\right)_x$			

defined irregular amorphous features (Figure 5). The entrained particles for the latter case were smaller in size (spanning a range between  $0.1$  and  $0.65 \mu\text{m}$  in size with a mean diameter of  $0.33 \mu\text{m}$ ).

The super-hydrophobicity of these plasma polymer coated glass slides was not found to deteriorate (age) over a period of 2 months (based on water contact angle and XPS analysis). In addition, the deposited nanospheres appear to be well-bonded to the substrate and also to each other.

## Discussion

The deposition of super-hydrophobic films by continuous plasma polymerization has been previously reported for  $2,2,3,3,4,4,4$ -heptafluorobutyl acrylate,<sup>5,24</sup>  $1,1,1,3,3,3$ -hexafluoroisopropyl acrylate,  $2,2,3,3,3$ -pentafluoropropyl acrylate, and ethyl heptafluorobutyrate.<sup>24</sup> In the current study, it has been shown that repetitive (rather than continuous) deposition of PFAC plasma polymer leads to the formation of well-defined perfluoroalkylated nanospheres that display super-hydrophobic attributes. This is in marked contrast to the irregular morphologies previously observed following pulsed plasma polymerization of fluoromonomers on the micro- to millisecond time scales.<sup>22,23,32</sup>

Powder formation and growth within plasmas are known to occur at relatively high pressures in association with high plasma energy densities.<sup>33–36</sup> This leads to the creation of large concentrations of condensable radicals and ions, as well as helping to lower the diffusion path lengths of reactive species contained within the plasma. Under these conditions gas-phase reactions between radicals and other species are fa-

(32) Labelle, C. B.; Gleason, K. K. *J. Appl. Polym. Sci.* **1999**, *74*, 2439.

(33) Yasuda, H. *Plasma Polymerization*; Academic Press: London, 1985.

(34) d'Agostino, R. *Plasma Deposition, Treatment, and Etching of Polymers*; Academic Press: London, 1990.

(35) Takahashi, K.; Tachibana, K. *J. Vac. Sci. Technol. A* **2001**, *19*, 2055.

(36) Hadjad, A.; Beorchia, A.; Roca I Cabarros, P.; Boufendi, L.; Huet, S.; Bubendorff, J. L. *J. Phys. D: Appl. Phys.* **2001**, *34*, 690.

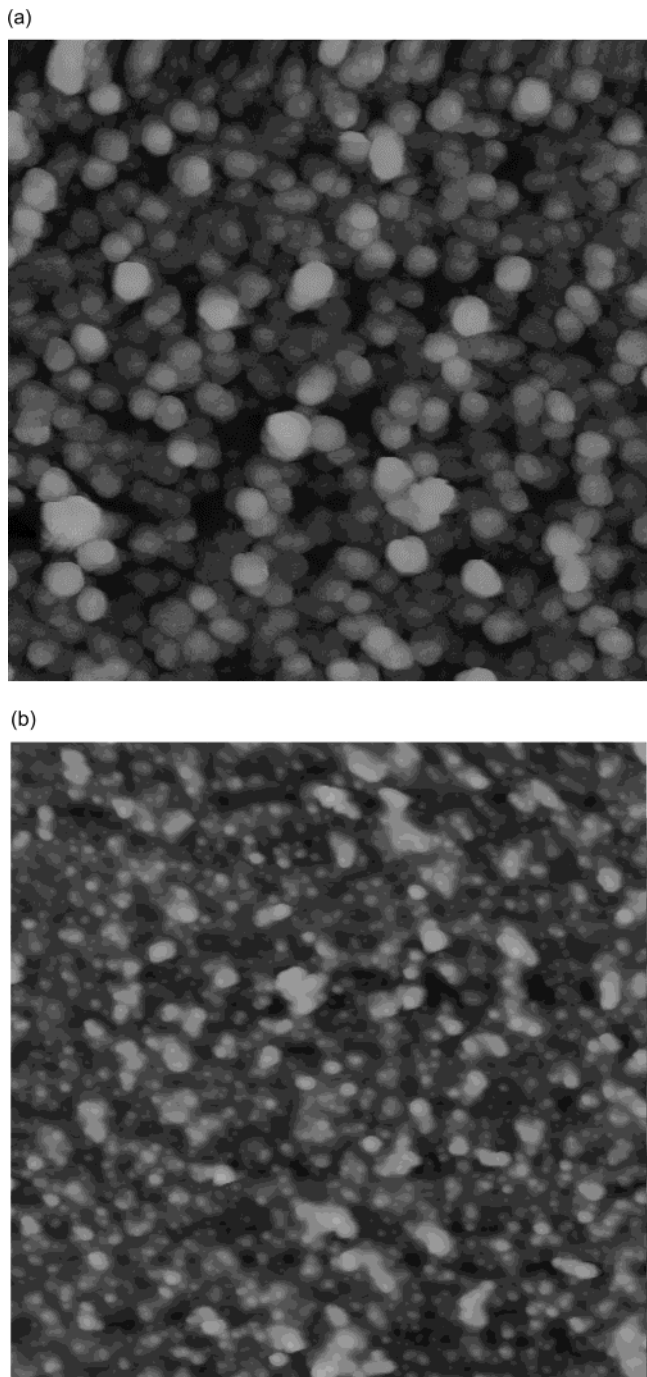


**Figure 5.**  $10 \times 10 \mu\text{m}$  AFM images of  $1\text{H},1\text{H},2\text{H},2\text{H}$  perfluoroctyl acrylate plasma polymer surface: (a)  $5 \times 1$  min repetitive bursts; and (b)  $1 \times 5$  min.

vored. Upon reaching a critical number density, rapid agglomeration is triggered,<sup>37</sup> culminating in powder deposition onto the underlying substrate surface due to gravitational effects. The short plasma bursts employed in the current investigation favor particle nucleation and growth during the on period, followed by particle deposition and monomer replenishment during the off period.<sup>38–40</sup> Whereas longer continuous wave plasma

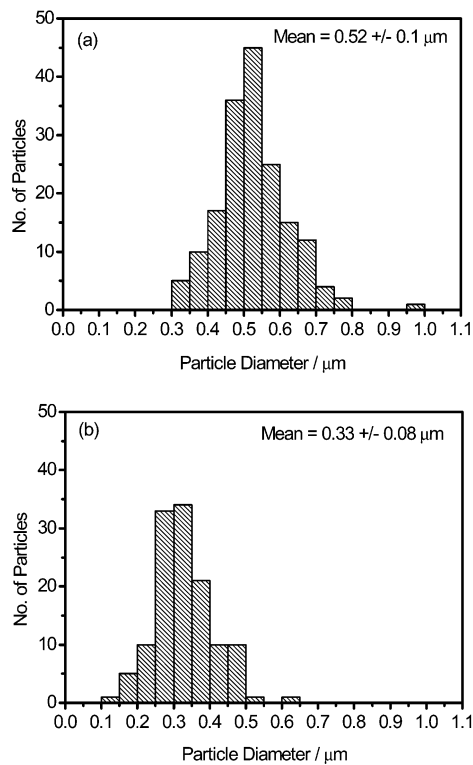


**Figure 6.** Particle size distribution from AFM micrographs: (a)  $5 \times 1$  min and (b)  $1 \times 5$  min.

deposition periods (e.g.  $1 \times 5$  min) produce excessive secondary products, causing the partial pressure of monomer to drop to an extent that precludes exclusive powder formation from the precursor, rather a mixed powder–film is deposited. Furthermore, surface etching is more likely. Modulating the plasma in the aforementioned manner helps to control the size of the deposited particles. This has also been successfully employed for the growth of nanostructured amorphous silicon films for optoelectronic applications.<sup>38</sup>

AFM analysis clearly shows the formation of nanospheres following short 1 min repetitive bursts of PFAC continuous wave plasma polymerization. Furthermore, XPS, FTIR, and ToF-SIMS surface analysis convey a high degree of monomer structural retention in these films (one notable exception being the slight loss of oxygen associated with the ester functionality). This can be attributed to the high monomer vapor pressure employed throughout this study helping to minimize the proportion of secondary side reactions. On the basis of AFM analysis, the nanosphere deposition is the same for each 1 min plasma burst. Therefore, the slight rise in contact angle values and  $(\text{CF}_2 + \text{CF}_3)$  group concentration with the increasing number of cycles (eventually reaching a steady state) can be attributed to monomer grafting onto underlying reactive sites generated during the previous 1 min pulse (the permeation of plasma species into porous structures is well-known<sup>41</sup>). This is in marked contrast to previous fluorocarbon plasma polymer particulate deposition studies where poor monomer structural retention was observed.<sup>35</sup>

(37) Hollenstein, C. *Plasma Phys. Control Fusion* **2000**, *42*, R93.

(38) Viera, G.; Huet, S.; Bertran, E.; Boufendi, L. *CIP 2001 Proceedings, 13th International Colloquium on Plasma Processes*; Antibes-Juan-les-Pins: France, p 160.

(39) Boufendi, L.; Herman, J.; Bouchoule, A.; Dubreil, B.; Stoffels, E.; Stoffels, W. W.; deGiorgi, M. L. *J. Appl. Phys.* **1994**, *76*, 148.

(40) Boufendi, L.; Plain, A.; Blondeau, J. P.; Bouchoule, A.; Laure, C.; Toogood, M. *Appl. Phys. Lett.* **1992**, *60*, 169.

(41) Godfrey, S. P.; Little, I. R.; Badyal, J. P. S. *J. Phys. Chem. B* **2001**, *105*, 2572.

In the case of water as the probe liquid, the measured low contact angle hysteresis is indicative of a composite surface.<sup>5,17</sup> The inherent surface roughness causes air to become trapped in voids (i.e. prevents liquid from penetrating), in accordance with the Cassie–Baxter relationship.<sup>42</sup> The contact angle hysteresis observed with *n*-decane is best described by the model of Johnson and Dettre,<sup>10</sup> i.e., the level of roughness is not sufficient for there to be a truly composite interface for this lower surface tension probe liquid (i.e. hysteresis prohibits super-oleophobic behavior for *n*-decane). The larger advancing contact angle value observed with *n*-decane for the 5 × 1 min plasma polymer surface compared to its 1 × 5 min counterpart is consistent with a greater surface roughness.

On the basis of the proposed mechanism, one would expect other monomers to behave in a similar fashion during repetitive continuous wave plasma polymerization, where the off-time should be sufficiently long for complete replenishment of precursor molecules and the on-time restricted to just the nucleation and growth

phase of particulates in the plasma (i.e. minimal secondary reaction processes). Apart from super-hydrophobicity, another potential application of these well-defined porous layers could be low permittivity materials<sup>35</sup> (e.g. interlayer dielectrics for ULSI circuits).

## Conclusions

Sequential short continuous wave bursts of PFAC plasma polymerization leads to the deposition of low surface energy nanospheres. These arise as a consequence of rapid monomer replenishment and minimal secondary reaction processes within the electrical discharge. Particle agglomeration gives rise to the formation of a composite surface that exhibits super-hydrophobicity (low water contact angle hysteresis). The corresponding films obtained by employing the same total on-time equivalent are found to be inferior.

**Acknowledgment.** We would like to thank DSTL for permission to publish Crown Copyright Material 2001-DSTL.

CM011600F

(42) Cassie, A. B. D.; Baxter, S. *Trans. Faraday Soc.* **1944**, *3*, 16.